

SIGNALS OF OPPORTUNITY P-BAND INVESTIGATION (SNOOPI) - MISSION OVERVIEW

M. Vega⁽¹⁾, J. Garrison⁽²⁾, R. Shah⁽³⁾, J. Mansell⁽²⁾, B. Nold⁽²⁾, J. Piepmeier⁽¹⁾, S. Kim⁽²⁾, J. Raymond⁽¹⁾, R. Bindlish⁽¹⁾, M. Kurum⁽⁴⁾, K. Horgan⁽¹⁾, K. Larsen⁽³⁾, R. Banting⁽¹⁾, D. Cody⁽³⁾, C. Kielbasa⁽¹⁾, M. Coon⁽¹⁾

¹ NASA GSFC, Greenbelt Maryland, United States

² Purdue University, West Lafayette Indiana, United States

³ NASA JPL, Pasadena California, United States

⁴ Mississippi State University, Starkville Mississippi, United States

ABSTRACT

The Signals of Opportunity P-band Investigation (SNOOPI) mission will be the first demonstration of measurements within the 240-380 MHz spectrum in a bi-static configuration from low earth orbit (LEO). The mission is a collaboration between Purdue, GSFC, JPL and MSU led by Purdue. P-band observations are expected to enable future root zone soil moisture (RZSM) and snow water equivalent (SWE) measurements derived from complex reflection coefficients obtained through the signals of opportunity (SoOp) technique.

Key objectives for the mission are as follows: 1) validation of the forward model under a wide variety of surface conditions and terrain, 2) assess radio frequency interference (RFI) from space and 3) validate functionality of the reflectometer instrument prototype with respect to uncertainties in source satellite position, transmitted power and predicted delay and Doppler values from the signal reflected.

This paper summarizes salient features applied to achieve key objectives with emphasis on the P-band reflectometer science instrument.

1 MISSION ARCHITECTURE

The SNOOPI mission architecture is divided into two categories, 1) the flight segment and 2) the ground segment. Figure 1 shows both segments as well as interfaces between and within. The flight segment comprises the observatory which is further divided into spacecraft bus and payload or reflectometer instrument. The reflectometer instrument is composed of four subsystems, 1) two deployable turnstile dipole antennas, 2) a low noise front end, 3) a digital back end and 4) a dual-band GPS receiving system. The spacecraft is divided into five primary subsystems, 1) command and data handling (CDH), 2) attitude control and determination system (ACDS), 3) power, 4) communications and 5) thermal management.

The ground segment is comprised of a science operations center (SOC) located at Purdue University, a mission operations center (MOC) at Goddard Space Flight Center (GSFC) with

support from ground assets managed by the Advanced Communications Capabilities for Exploration and Science Systems (ACCESS) project [1]. Although not shown in Figure 1, the ground segment will also include a power and ambiguity function monitor station to be deployed at Purdue [2].

A science team led by Purdue with contributions from GSFC, JPL and MSU will be responsible for algorithm evaluation. Over 40 matchups with SMAP cal/val sites are expected over a 9-month science campaign [3].

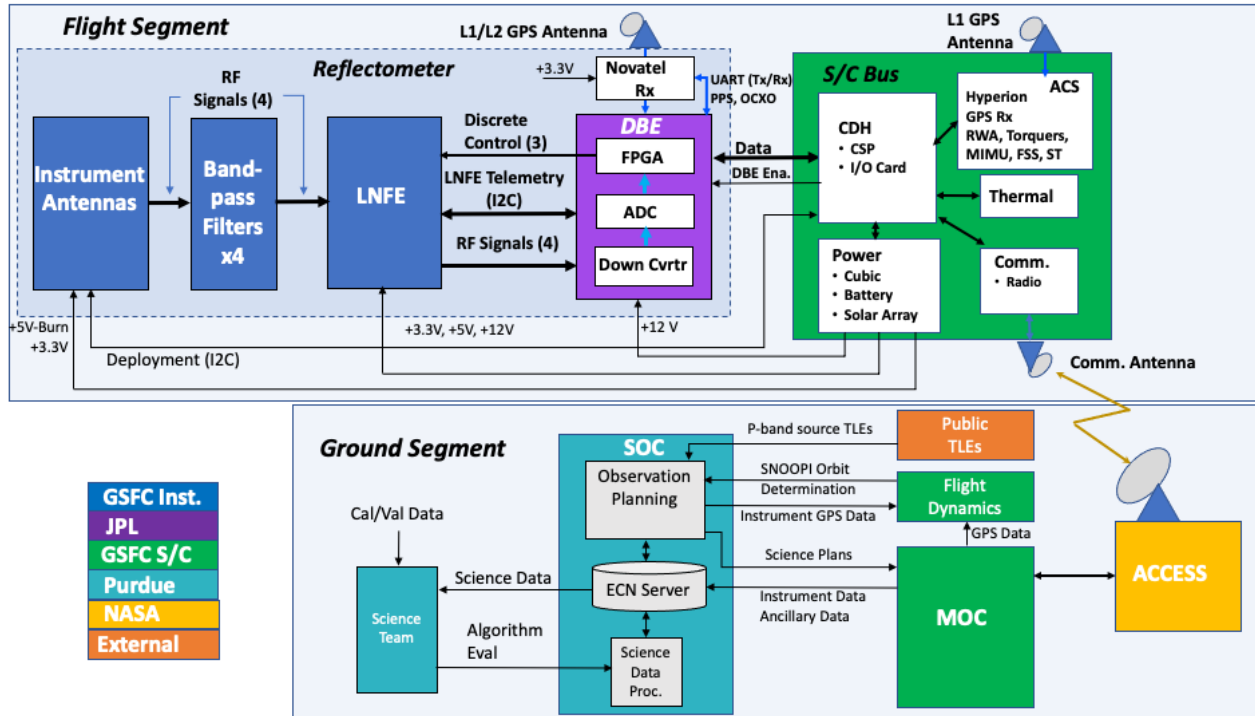


Figure 1. SNOOPI mission architecture diagram.

1.1 OBSERVATORY

The SNOOPI observatory was designed in a 6U (3 x 2) cubesat form factor compatible with a NanoRacks deployer from the International Space Station (ISS). Thus it is planned for launch during a cargo resupply mission for release into an orbit of ~400 km altitude with 51.6 deg inclination. Figure 2 shows a computer-aided design (CAD) rendering of SNOOPI. Deployable science payload dipole antennas are placed at each end (top and bottom), L1 and L1/L2 GPS antennas are placed on the zenith pointing or top end, S-band communications antennas (not visible in Figure 2) are placed in the nadir and back facing sides. Science payload antenna placement was inverted (long dipoles on bottom side and short dipoles on top side) to optimize expected performance after critical design review, but it is not depicted in Figure 2.

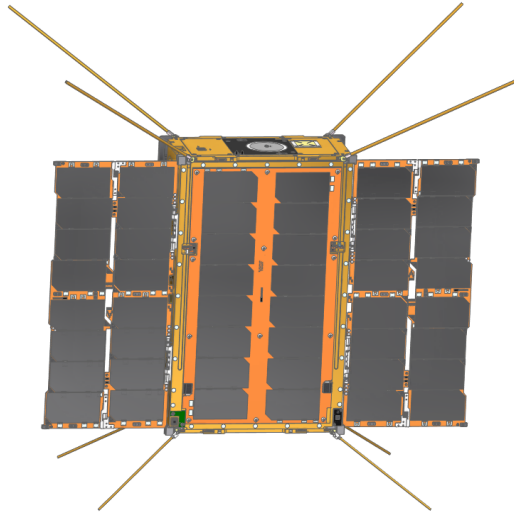


Figure 2. Rendering of the SNOOPI observatory.

2 REFLECTOMETER INSTRUMENT

SNOOPI's payload is a P-band reflectometer instrument comprised of four subsystems. Namely, a low noise front end (LNFE), digital back end (DBE), antennas (ANT) and an L1/L2 global navigation satellite system (GNSS) receiving unit. Figure 3 shows the instrument architecture with interfaces and salient features. Table 1 summarizes instrument parameters. Figure 5 shows the integrated instrument stack.

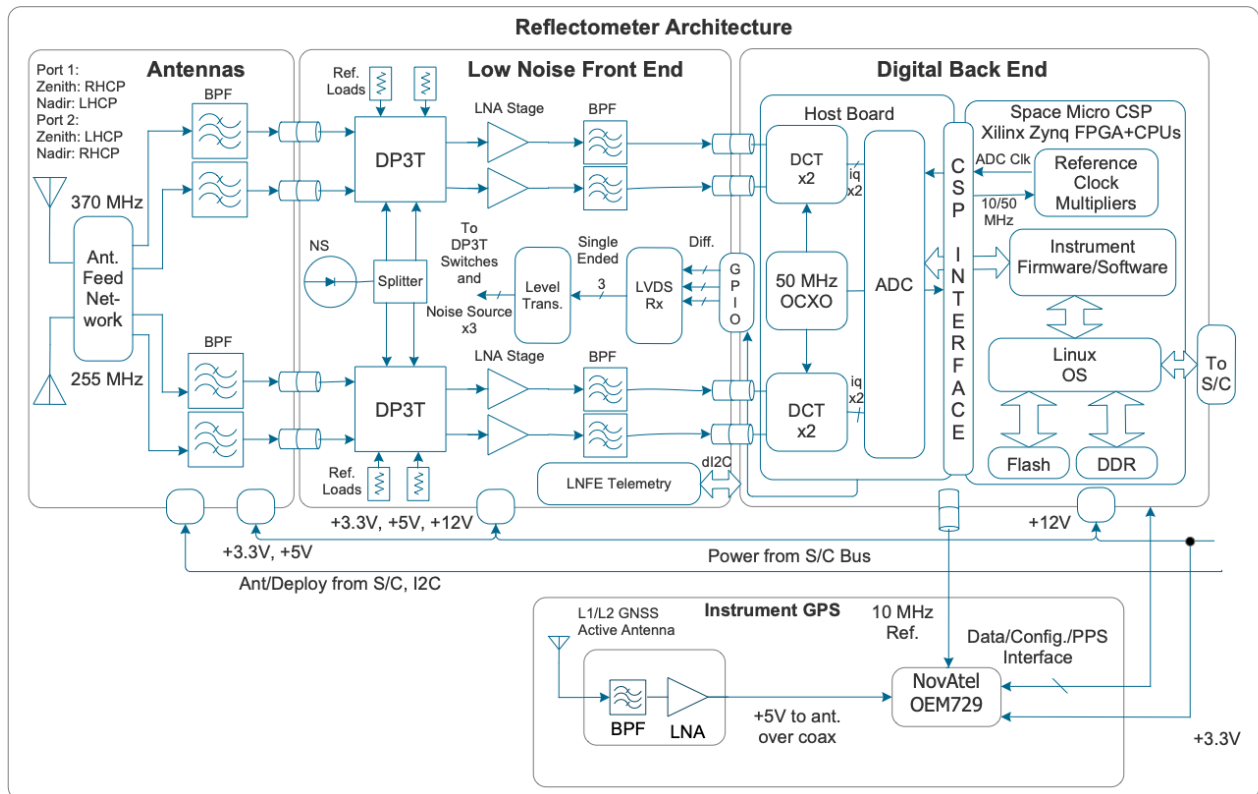


Figure 3. SNOOPI reflectometer instrument architecture diagram.

Table 1. SNOOPI instrument parameters.

	High Band	Low Band
Center Frequency (antennas)	370 MHz	255 MHz
Polarization	Primary – RHCP/LHCP (Zenith/Nadir) Backup - LHCP/RHCP (Zenith/Nadir)	Primary – RHCP/LHCP (Zenith/Nadir) Backup - LHCP/RHCP (Zenith/Nadir)
Modulation Bandwidth	5 MHz	25 kHz
Coherent Integration Time	2 ms (default)	2 ms (default)
Chip Length	60 m	12 km
Delay Resolution	0.25 chip	0.05 chip
Delay Bins	200	5
Doppler Resolution	250 Hz	250 Hz
Doppler Bins	3	3
Number of Channels	1	5
Primary Operation Mode (high/low band primary and backup antenna ports selectable)	Delay-Doppler Mapping	Delay-Doppler Mapping
Additional Operation Modes (limited to a single antenna port per data capture)	Filtered IF (5 MHz bandwidth), Raw IF (25 MHz bandwidth centered at 370 MHz, 50 Msps)	Filtered IF (35 kHz bandwidth, 500 ksps, x5 channels), Raw IF (50 MHz bandwidth centered at 270 MHz)

2.1 Antennas

The SNOOPI antennas are minimally customized versions of a standard product design with heritage in cubesat VHF and UHF communication applications. Customizations performed were the retuning per mission frequency band requirements listed in Table 1. Each antenna is composed of four rods along with matching networks to form circularly polarized radiation patterns. Rods are stowed along the cubesat body and deployed by melting of burn wires (in Figure 2). Each antenna is equipped with two ports corresponding to RHCP (zenith), LHCP (nadir) and LHCP (zenith), RHCP (nadir) polarizations. Figure 4 shows radiation patterns for the primary ports. The LHCP (zenith), RHCP (nadir) ports are reserved as backups. These can be used as redundant channels with proper spacecraft rotations. The antennas are followed by band limiting filters (in Figure 3). These filters protect the receiver against damage from powerful ground-based radar transmitters operating within the VHF and UHF bands as well as from saturation given the antennas are expected to have resonant modes at higher frequencies.

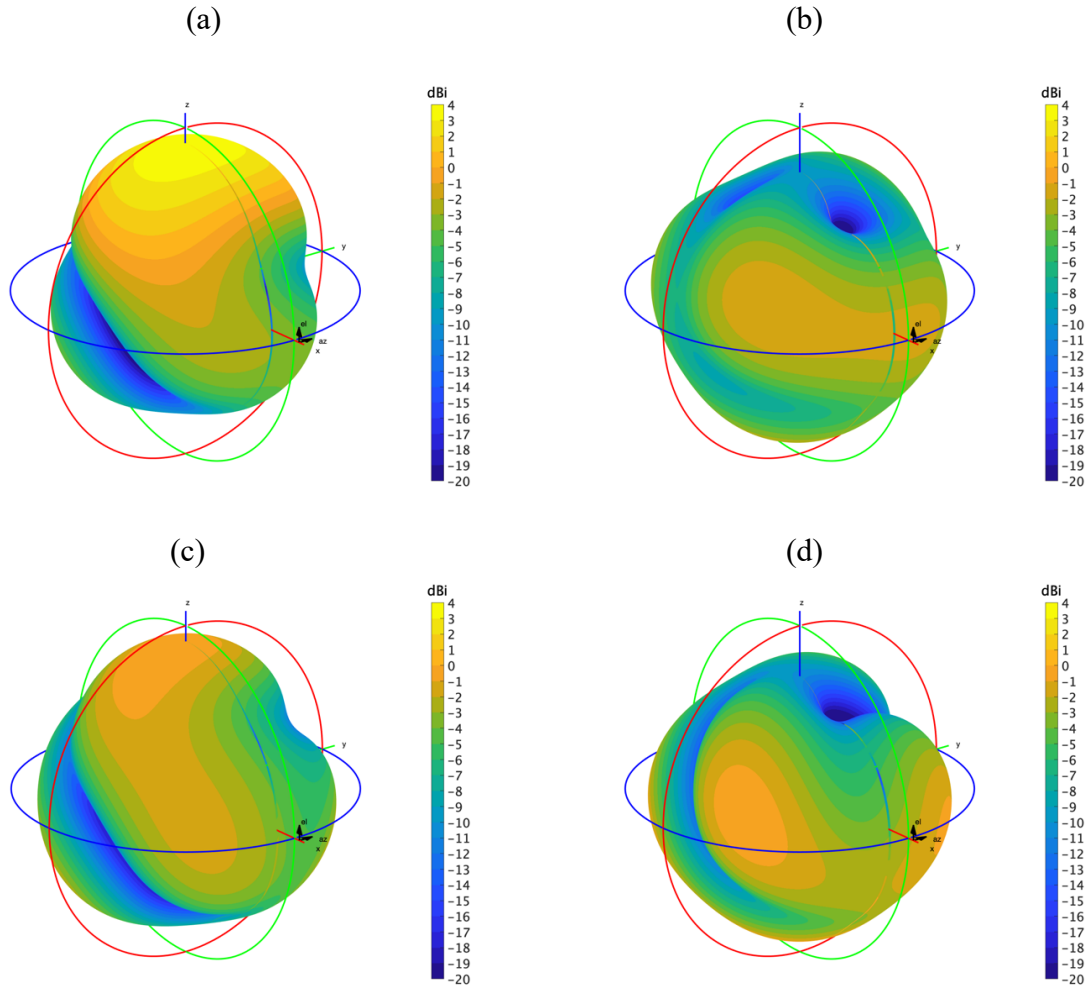


Figure 4. SNOOPI reflectometer antenna patterns, low band (a) RHCP (b) LHCP and high band (c) RHCP, (d) LHCP.

2.2 Low noise front end

The LNFE is a custom build by GSFC with heritage from the SoOp airborne demonstrator (SoOp-AD) [4] and other internal investments leading towards miniaturization for cubesat applications. It provides low noise amplifying stages as well as filtering stages to mitigate re-entrant bands exhibited by filters used prior. A pair of double-pole triple-throw (DP3T) switches provide the capability to inject broadband noise signals from temperature monitored loads and a noise source. These will be used to track receiver gain variations over temperature. A power limiter is also included to protect the downconverters embedded within the digital back end. Temperature telemetry is handled through a custom built card containing pre-conditioning and a 16-bit analog to digital converter (ADC).

2.3 Digital back end

The DBE was developed and provided by JPL. It has extensive heritage from previous missions. The primary components are a SpaceMicro CubeSat Processor (CSP) together with a custom designed RF/clock host card. Four downconverters together with eight 14-bit analog to digital converters and field programmable gate array (FPGA) resources are used to map incoming P-band signals to baseband prior to delay-Doppler map (DDM) processing. A high performance oven-controlled crystal oscillator (OCXO), also included within the DBE, is used to phase-lock downconverters, generate sampling and GNSS receiver clocks among others. The DBE also provides control signals for the DP3T switches within the LNFE and records temperature telemetry through an I2C interface. Table 1 summarizes operation modes.

2.4 GNSS receiver

Lastly, the GNSS receiving unit is based on a commercially available card by Novatel, packaged and qualified at GSFC. The unit interfaces with the DBE to provide timing to the reflectometer. A selection of data logs including housekeeping telemetry and pseudoranges are recorded and embedded within the DBE data stream. GPS L1 and L2 frequencies will be used for improved orbit determination.

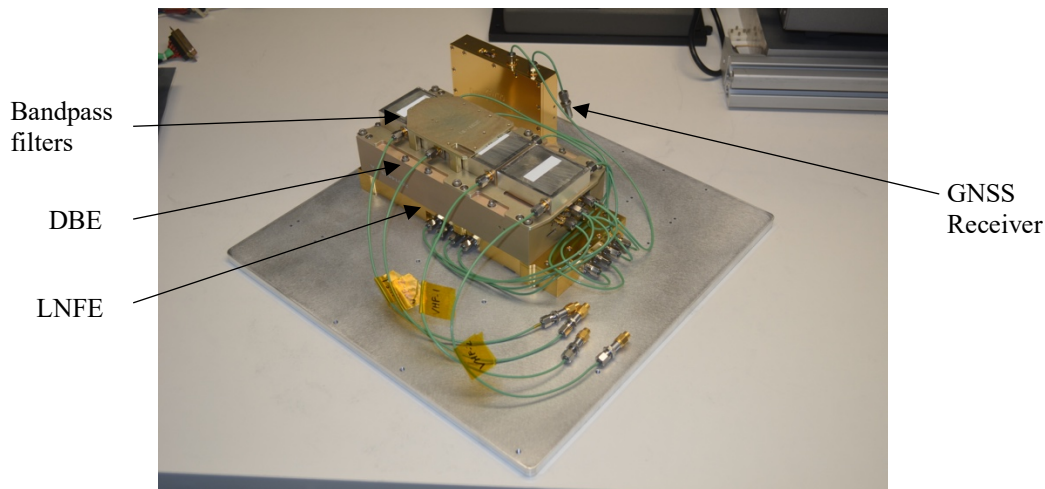


Figure 5. SNOOPI instrument stack on integration and testing handling jig.

2.5 Integration and testing (I&T) activities

The SNOOPI instrument has undergone an extensive integration and testing phase prior to delivery to observatory I&T. Throughout, the primary focus was in verification of functionality and hours of operation in a representative thermal environment. Numerous tests, updates and thermal cycles were performed (including thermal cycles at sub-assembly level). Figure 6 shows the power spectral density (PSD) obtained from a raw data capture performed during a live sky test in Nov 18th of 2021 at GSFC facilities, in Greenbelt, MD. Raw mode data captures allow for examination of the entire instrument spectrum of interest. In the case shown, the PSD corresponds to the instrument high band which is centered at 370 MHz and encompasses frequencies from 345 to 395

MHz (-25 to 25 MHz in figure). A few things of note in Figure 6, first, the instrument shows sensitivity to the incoming signals of interest, four MUOS, 5 MHz channels centered around the PSD 0 Hz mark corresponding to 370 MHz. Even though the test setup (in Figure 7) used a vertically polarized log-periodic antenna with higher gain compared to the flight antennas, there were several losses that make the measurement comparable (e.g. polarization loss, cable loss, 4-way splitter loss). Second, a significant amount of radio frequency interference (RFI) is seen peaking near 380.27 MHz (10 MHz in Figure 6). Such signals appear to be related to land mobile and aviation radios, which are expected to be heavily attenuated given the space loss from ground to LEO orbit. However, they do add some complexity while conducting ground testing.

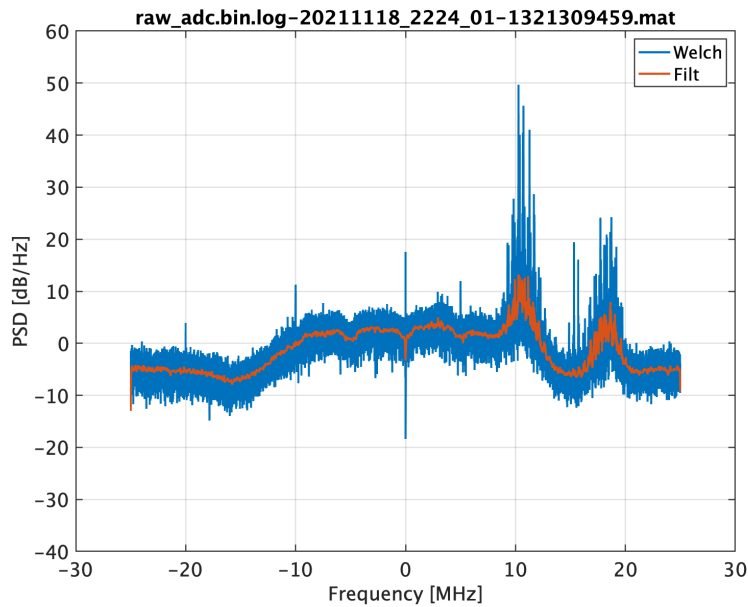


Figure 6. High band spectrum from raw IF data capture during outdoor live sky test.



Figure 7. Live sky instrument test setup.

Another test performed during instrument I&T was the injection of a test signal resembling spectral density, delay and Doppler values expected on orbit. Figure 8 shows an example delay-Doppler map from this test. The simulated delayed replica was shifted by 1 ms and 2440 Hz, which correspond to a peak near the center as in Figure 8.

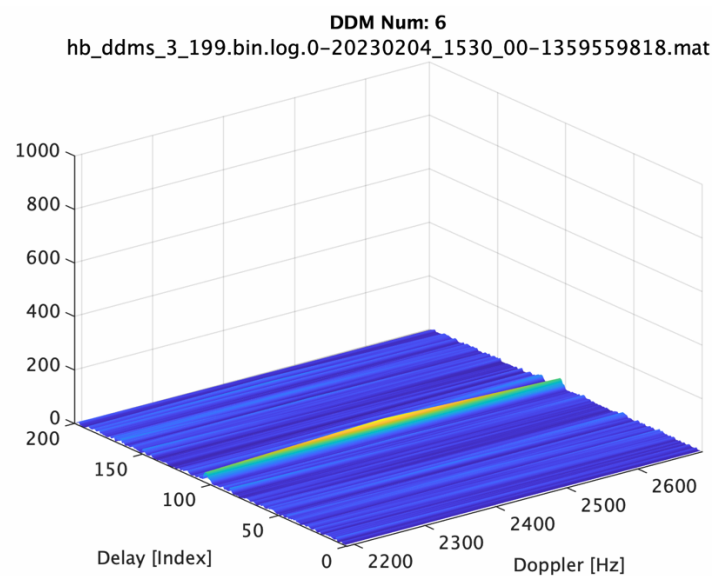


Figure 8. High band delay-Doppler map from simulated input test signal.

3 CONCLUSIONS

A summary of the SNOOPI mission architecture to meet its key objectives was described. Emphasis was placed on the mission payload, the SNOOPI reflectometer instrument. Salient features of its architecture were discussed along with a summary of specifications. A brief discussion of I&T activities and results was also provided.

4 ACKNOWLEDGEMENTS

The SNOOPI mission is funded by the NASA Earth Science Technology Office (ESTO) In-Space Validation of Earth Science Technologies (In-VEST) program. The authors acknowledge great contributions from team members including, but not limited to Austin Tanner/GSFC and Paul Lestingi/GSFC.

5 REFERENCES

- [1] J. L. Garrison et al., "SNOOPI: Demonstrating P-Band Reflectometry from Orbit," 2021 IEEE International Geoscience and Remote Sensing Symposium IGARSS, 2021, pp. 164-167, doi: 10.1109/IGARSS47720.2021.9554546.
- [2] B. Nold et al., "Design of a Ground Based Power and Ambiguity Function Monitor for P-Band Signals of Opportunity Sources," 2022 IEEE International Geoscience and Remote Sensing Symposium IGARSS, 2022
- [3] Garrison et al., "Instrument Science Experiments on the SNOOPI P-band Reflectometry Mission," 2022 IEEE International Geoscience and Remote Sensing Symposium IGARSS, 2022
- [4] J. Knuble et al., "Airborne P-band Signal of Opportunity (SoOp) demonstrator instrument; status update," 2016 IEEE International Geoscience and Remote Sensing Symposium (IGARSS), 2016, pp. 5638-5641, doi: 10.1109/IGARSS.2016.7730473.